

Stripe structure, spectral feature and soliton gap in high T_c cuprates

Kazushige Machida, and Masanori Ichioka

Department of Physics, Okayama University, Okayama 700-8530, Japan

(November 6, 2017)

We show that the lightly doped $\text{La}_{2-x}\text{Sr}_x\text{CuO}_4$ can be described in terms of a stripe magnetic structure or soliton picture. The internal relationship between the recent neutron observation of the diagonal ($x=0.05$) to vertical ($x \geq 0.06$) stripe transition, which was predicted, and the concomitant metal-insulator transition is clarified by this solitonic physics. The phase diagram with the unidentified transition lines between antiferromagnetic to stripe phases, the doping dependence of the modulation period, the origin of the mid-infrared optical absorption are investigated comparatively with other single layer systems: $\text{La}_{2-x}\text{Sr}_x\text{NiO}_4$ and $(\text{La},\text{Nd})_{2-x}\text{Sr}_x\text{CuO}_4$. The novel type of quasi-particles and holes is fully responsible for metallic conduction and ultimately superconductivity.

PACS numbers:74.25.-q,75.25.+z,75.60.Ch

Much attention has been focused on electronic properties in underdoped high T_c cuprates recently because it is hoped that understanding of the unusual ground state may lead us to a clue to a high T_c mechanism. However, in spite of intensive theoretical and experimental works in the past little consensus for the normal state properties has emerged yet.

Recently a remarkable series of elastic neutron experiments [1–3] on $\text{La}_{2-x}\text{Sr}_x\text{CuO}_4$ (LSCO) has been performed, revealing static magnetic incommensurate (IC) structure: (1) For $x=0.12, 0.10, 0.08$ and 0.06 , which are all metallic and superconducting, the modulation vector \mathbf{Q} are characterized by $\mathbf{Q} = (\frac{1}{2}, \frac{1}{2} \pm \epsilon)$ and $(\frac{1}{2} \pm \epsilon, \frac{1}{2})$ in reciprocal lattice units (r.l.u.). The IC modulation runs vertically in the a (b)-axis of the CuO_2 plane. (2) For $x=0.05$ which is insulating the above four superspots rotate by 45° around the $(\frac{1}{2}, \frac{1}{2})$ position, characterized by $(\frac{1}{2} \pm \epsilon, \frac{1}{2} \pm \epsilon)$. The IC modulation is now in the diagonal direction. (3) The incommensurability ϵ is given by $\epsilon = x$ for $0.05 \leq x \leq 0.12$ beyond which ϵ saturates (see Fig.2). (4) For $x=0.03$ and 0.04 the elastic peaks are also observed at the commensurate (C) position, but the peak profiles are abnormally broaden, suggesting that the IC modulation is hidden. The static nature of these orderings at low T 's are also corroborated by μSR measurement [4].

These lightly doped systems were known to be in spin-glass region ($0.02 \leq x \leq 0.05$). In the further dilute region ($0 < x \leq 0.02$) upon lowering T the antiferromagnetic (AF) phase changes into a “spin-freezing” structure at the Johnston line given by $T_f=815x$ (K), below which the internal magnetic field probed by the La-NQR is mysteriously broaden [5]. This transition line will be interpreted differently below.

Prior to these experiments, there has been known the static magnetic structures in superconducting $(\text{La}, \text{Nd})_{2-x}\text{Sr}_x\text{CuO}_4$ (Nd) and insulating $\text{La}_{2-x}\text{Sr}_x\text{NiO}_4$ (Ni). In the former Nd system [6] the vertical stripe with the same $\epsilon = x$ relation as in LSCO for $x > 0.07$ and in the latter Ni system the diagonal stripe with $\epsilon = x/2$ up to $x \simeq 0.33$ are observed [7]. Note that in $\text{YBCO}_{6.6}$ verti-

cal IC fluctuations are also reported in inelastic neutron experiments [8].

Almost a decade ago one of the authors [9,10] predicts some of the above features of the static IC spin modulation in lightly doped cuprate systems, stressing the charged stripe or the solitonic structure as a convenient and universal “vehicle” to accommodate excess carriers in an otherwise commensurate antiferromagnet within a mean-field treatment for a simple two-dimensional Hubbard model. Some features of them were independently found by others [11] at that time and are now confirmed by a more sophisticated method, such as DMRG [12]. Specifically we have predicted [9,10]: (1) The diagonal to vertical transition occurs as doping proceeds. (2) The incommensurability ϵ is given by $\epsilon = n_h/2$ where n_h is the hole density per site and proportional to x . In other words, once holes are introduced in CuO_2 plane the ground state is always described by a modulated IC structure. (3) The newly created solitonic midgap band situated between the insulator main gap accommodates excess carriers, keeping the AF formation energy intact. The band width of the midgap state for the vertical stripe is wider than for the diagonal stripe, implying that the former (latter) has a tendency toward a metal (insulator).

Encouraged by the success of our predictions, we now further extend it to a slightly more realistic case: namely, we introduce a next nearest neighbor hopping t' to describe the metallic situation, which is certainly important to mimic the actual Fermi surface topology [13]. (The previous solutions with only the nearest neighbor hopping t were all insulating and fail to describe a metallic state [9–11].) Thus the main purpose of this paper is to establish the solitonic picture to resolve various mysteries or paradoxes in lightly doped regions, mainly focusing on LSCO. These include (A) why the metal-insulator transition and the diagonal-to-vertical transition occur simultaneously at $x \simeq 0.05$, (B) why the spin freezing ($0 < x < 0.02$) below the Johnston line and the spin-glass regions exist, and (C) why the midgap state observed by the mid-infrared optical absorption [14] grows progres-

sively with x . Here we are going to give a self-consistent picture based on soliton physics, which is quite different from an influential idea of frustrating charge segregation by Emery et al [15].

We start out with the standard Hubbard model $H = -\sum_{i,j,\sigma} t_{i,j} c_{i,\sigma}^\dagger c_{j,\sigma} + U \sum_i n_{i,\uparrow} n_{i,\downarrow}$ in two dimensions where $t_{i,j} = t$ for the nearest neighbor pairs (i, j) and $t_{i,j} = t'$ for the next nearest neighbor pairs situated on a diagonal position in a square lattice. (The energy is measured by t and $t'/t = -0.1$ and $U/t = 3.0$ are chosen in the following.) The mean field $\langle n_{i,\sigma} \rangle = n_i + \sigma M_i$ at i -site is introduced where $n_i (M_i)$ is the charge (spin) density. Thus the one-body Hamiltonian $H_{MF} = -\sum_{i,j,\sigma} t_{i,j} c_{i,\sigma}^\dagger c_{j,\sigma} + U \sum_i (\langle n_{i,\uparrow} \rangle n_{i,\downarrow} + \langle n_{i,\downarrow} \rangle n_{i,\uparrow})$ is solved self-consistently in k -space under a given hole concentration or filling $1 - n_h$ per site ($n_h=0$ is just the half-filling), assuming a spatially periodic structure for spin and charge modulations with $\epsilon = n_h/2$.

The resulting phase diagram in T vs n_h is displayed in Fig.1 where the simple commensurate AF state denoted by C is never stable at $T=0$. Upon raising T the vertical incommensurate (VIC) or the diagonal incommensurate (DIC) phase are crossed-over to the AF because of an entropy effect. These spatially modulated spin structures or soliton structures are characterized by a periodically placed π -shifted domain wall (or a kink) which neatly accommodates excess carriers. The charge carriers align perpendicularly to $\mathbf{Q} - (\frac{1}{2}, \frac{1}{2})$ (see Fig.1 in Ref. [10]). The transition from DIC to VIC upon increasing n_h can be understood as arising from the competitive effects between the nesting of \mathbf{Q} -vector ($\frac{1}{2} \pm \epsilon, \frac{1}{2} \pm \epsilon$) in DIC at low doping and gapping at the $(1, 0)$ saddle point position with large density of states in VIC. Note that the nesting deteriorates with n_h , necessarily inducing DIC to VIC transition.

The Johnston line $T_f = 815x$ (K) for $0 < x \leq 0.02$ which indicates the anomalous broadening of the La resonance line [16] thus named a spin freezing T_f , signals the change of the internal magnetic field distribution. It may correspond to the C-IC transition line in Fig.1. Although the present numerical calculation gives it a first order, actual transition is of second order (see the detailed analytical discussions in Ref. [9]). According to Fig.1 the known spin-glass region ($0.02 \leq x \leq 0.04$) is also described by the DIC structure. Indeed the recent neutron [1-3] and μ SR [4] experiments suggest this is the case as mentioned above. Previous spin-glass identification simply reflects dirt effects.

The incommensurability ϵ is calculated as $\epsilon = n_h/2$ near half-filling at $T=0$. The reduced k -space area spanned by this \mathbf{Q} -vector is exactly filled by excess holes, differing from the simple so-called $2k_F$ -instability in one-dimensional case (k_F the Fermi wave number). It means that the charge stripe is completely filled with holes, never stabilizing the “half-filled” stripe in our calcula-

tions [17]. This is in sharp contrast with Tranquada’s claim for Nd systems [6]. The observed ϵ is precisely given by $\epsilon = x$ both for LSCO and Nd systems at low doping levels of $x \lesssim 0.12$. This implies $\epsilon = n_h$ which corresponds to a half-filled stripe if we identify $n_h = x$. The observation $\epsilon = x$ is also contrasted with the neutron result $\epsilon = x/2$ for Ni systems [7], which does agree with our estimate. This “factor 2” paradox in LSCO and Nd is quite intriguing and may be important in evaluating the actual hole concentration in CuO_2 plane. Here we suggest a possible scenario to resolve it: Fig.2 shows the observed data of ϵ for three systems (filled symbols) and n_{eff} (open ones) estimated by Uchida et al [14] through optical conductivity measurements. It is seen that according to Uchida’s data under a given x the supplied n_{eff} in CuO_2 is doubled for LSCO and Nd compared to Ni at least for $x \leq 0.1$. This immediately resolves the above paradox, namely, $n_h = 2x$ for LSCO and Nd. The theoretical relation $\epsilon = n_h/2$ is valid for all three systems commonly and there is no half-filled stripe. It is noted, interesting enough, from Fig.2 that a precise coincidence between ϵ (filled circles) and n_{eff} (open circles) against x is seen to be hold even beyond $x \sim 0.12$ up to $x \sim 0.25$ for LSCO and Nd. It means that beyond $x \sim 0.12$ doped holes do not come into the relevant magnetic band.

The spatial magnetic structure is characterized by a soliton form with many higher harmonics of the Fourier components of the order parameters; M_{lQ} (spin) and n_{lQ} (charge). The period of the charge density is half that of the spin density. The tending limits of those toward $n_h \rightarrow 0$ (half-filling limit) are given by $M_{(2l+1)Q}/M_Q \rightarrow \frac{1}{2l+1}$, $M_Q/M_C \rightarrow \frac{2}{\pi}$ and $n_{2lQ} \rightarrow 0$ ($l = 1, 2, 3, \dots$) where M_C is the AF order parameter. That is, the spin modulation becomes a squaring-up cnoidal wave form, far from a simple sinusoidal one and the charge modulation becomes irrelevant when $n_h \rightarrow 0$. These features well coincide with the previous analytic solution $sn(x, k)$ for $t'=0$ [9].

Fig.3 shows the band structures for VIC and DIC. The original single band is fold back into the small reduced zone. In the AF case at half-filling the large main gap separates it into the filled and empty bands. The doping creates a new band or the soliton band, seen from Fig.3, in between the AF gap whose magnitude is relatively intact upon doping (also see Fig.7 in Ref. [10]). In DIC the midgap band is empty to accommodate holes and situated above the chemical potential $\mu (= 0)$. The midgap band width for VIC is substantially wider than that for DIC. In VIC the dispersive midgap band touches μ , making it metallic since the doping increases the soliton band width.

In Fig.4 the one-particle spectral weight is shown on the energy vs wave number plane along the symmetry lines for a metallic state: The reorganized band opens a large gap at $(0, 1)$ and $(-\frac{1}{2}, \frac{1}{2})$ positions where the soli-

tonic midgap band also situates. The hold-backed bands get spectral weight toward $(-1,1)$ direction after taking a plateau at $(0,1)$. This characteristic feature here is strikingly similar to that observed by photoemission experiments [13]. The midgap band creates “quasi-particles” in its bottom at $(0,1)$ and simultaneously the valence band also produces the same amount of “quasi-holes” at the valence band top at $(-\frac{1}{2}, \frac{1}{2})$. These newly created quasi-particles and -holes are mobile, fully responsible for metallic conduction and ultimately superconductivity. The Fermi surface pockets for these novel quasi-particles and holes are situated around the $(0,1)$ and $(-\frac{1}{2}, \frac{1}{2})$ position respectively in the Brillouin zone. The spectral weight has a two-fold symmetric form. The midgap band does not touch $\mu(=0)$ at $(1,0)$.

The aligned holes in VIC on a wall move easier than in DIC because of the difference of the effective hoppings (vertical vs diagonal hopping processes), resulting in the different effective masses for two soliton bands. The band dispersion is very anisotropic; the effective mass perpendicular to the \mathbf{Q} -vector is much heavier than that parallel to the \mathbf{Q} -vector. The holes localized on a wall are mobile only along the domain wall, once metallicity is attained upon doping. These make VIC more metallic while DIC insulating. In fact in our calculation in Fig.1 VIC (DIC) just corresponds to a metal (insulator), as coinciding with the observation [1,2]. However, we remark that the exact one-to-one correspondence is not generic, but the tendency that VIC is easier to become metallic than DIC is generic, independent of the choice of t' . Note that Ni systems are all DIC [7] and insulating, and Nd for $x > 0.07$ [6] and YBCO_{6.6} [8] are all VIC and metallic, agreeing with this general rule.

In Fig.5 we show the optical conductivity for two dopings. As n_h increases, the newly created midgap absorption from the valence (conduction)-to-soliton band transition process progressively grows inside the main AF gap at $\omega \sim 1.7$. Its area corresponds to the hole concentration. These characteristics agree with the common optical observations for all three systems [14]. The long-standing mystery of the origin of the mid-infrared absorption can be attributed to the soliton band.

In conclusion, we have found: (1) The metal-insulator transition (MIT) is accompanied by the profound magnetic structural change from the diagonal to vertical stripes as x increases. Note, however, that the actual MIT may be more complicated in the sense that the \mathbf{Q} vector may change gradually, resulting in a second-order like MIT. It is interesting to carefully trace the superspots in neutron experiment for the critical concentration of $x=0.05$ under varying T. (2) The incommensurate spin modulation persists down to $x \rightarrow 0$ at T=0, even deeply into the known “commensurate” ($0 < x \leq 0.02$) and spin glass regions ($0.02 < x \leq 0.04$) under the assumption that the doped holes spread out the whole sample without any defects or impurities. We point

out a possibility that the Johnston line may signal this commensurate-incommensurate transition. (3) The solitonic midgap band formed upon doping is responsible to the so-called mid-infrared absorption in optical conductivity measurements. (4) The incommensurability ϵ ; deviation from $(\frac{1}{2}, \frac{1}{2})$ position is linear in the hole concentration n_h per site at least in lightly doped region, coinciding with the recent neutron observation by Endoh and Yamada group [1–3].

Finally we remark that judging from the optical data of the main insulating gap (Ni \sim 4eV and LSCO \sim 2eV) the Ni system may have larger U than in LSCO [14]. This makes DIC in Ni stabler, keeping the system insulating up to higher doping level ($x > 0.33$) (see Fig.5 in Ref. [10] where the critical concentration of the DIC-VIC transition is shown to increase with x). This may be one reason why heavily doped nickelates remain insulating. As for Nd system we predict a similar 45° rotation of superspots in neutron experiments and concomitant metal-insulator transition at lower dopings. If these predictions are indeed confirmed experimentally, the present soliton picture must be a proper starting point to begin with in order to consider a high T_c mechanism.

The authors thank many colleagues for enlightening discussions on the most recent updated experiments, including Y. Endoh, K. Yamada, S. Wakimoto, H. Kimura, K. Hirota, S. Uchida, A. Fujimori, A. Ino, J. Tranquada, M. Arai and M. Matsuda.

-
- [1] S. Wakimoto, et al, preprint for $x = 0.03, 0.04, 0.05$.
 - [2] S. Wakimoto, et al, preprint for $x = 0.06$.
 - [3] T. Suzuki, et al, Phys.Rev.B**57**,R3229 (1998) for $x = 0.12$ and earlier references cited therein.
 - [4] Ch. Niedermayer, et al, Phys.Rev.Lett.**80**, 43843 (1998). They claim the similar phase diagram for YBCO.
 - [5] J.H. Cho, et al, Phys.Rev.Lett.**70**,222 (1993) and F.C. Chou, et al, ibid **71**,2323 (1993).
 - [6] J.M.Tranquada, et al, Phys. Rev. Lett. **78**,338 (1997) and earlier references cited therein.
 - [7] See reviews: J.M. Tranquada, cond-mat/9802043 and preprint (BNL-65377).
 - [8] H. Mook, et al, Nature **395**,580 (1998) and cond-mat/9811100. M. Arai, private communication.
 - [9] K. Machida, Physica C**158**,192 (1989).
 - [10] M. Kato, et al, J.Phys.Soc.Jpn.**59**, 1047 (1990).
 - [11] D. Poilblanc and T.M. Rice, Phys.Rev.B**39**,9749 (1989). J. Zaanen and O. Gunnarsson, ibid **40**,7391 (1990). H. Schulz, Phys.Rev.Lett.**64**,1445 (1990).
 - [12] S. White and D. Scalapino, Phys.Rev.Lett.**80**,1272 (1998).
 - [13] A. Ino et al, preprint, who are just revealing the detailed Fermi surface information in underdoped LSCO.
 - [14] S. Uchida, et al, Phys.Rev.B**43**,7942 (1991) for LSCO. T.

Ido, et al, Phys.Rev.B44,12094 (1991) for Ni. S. Uchida, private communication.

- [15] See for example, V.J. Emery, et al, Phys.Rev.B56,6120 (1997).
 [16] See B.J. Suh, et al, Phys.Rev.Lett.81,2791 (1998) for L-doped LSCO.
 [17] Also see, J. Zaanen and A.M. Oleś, Ann. Phys. 5, 224 (1996). T. Mizokawa and A. Fujimori, Phys.Rev.B56, 11920 (1997).
 [18] T. Arima, et al, Phys.Rev.B48,6597 (1993).

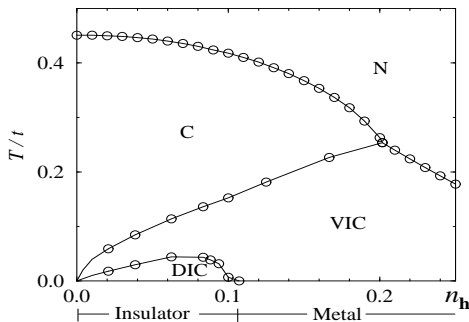


FIG. 1. Phase diagram in T vs n_h . C: antiferromagnetic VIC:vertical, and DIC: diagonal incommensurate phases. VIC (DIC) is metallic (insulating) at $T=0$. Note that $n_h = 2x$ for LSCO.

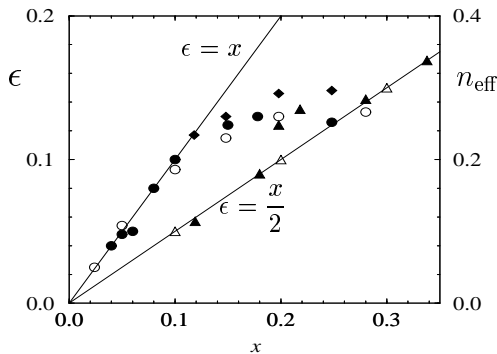


FIG. 2. Incommensurability ϵ vs doping x (left scale). $\epsilon = x$ for LSCO [1,2] (filled circle) and Nd [6] (diamond). $\epsilon = x/2$ for Ni [7] (filled triangle). The effective hole density n_{eff} vs x (right scale) estimated by Uchida [14] (open circle: LSCO, open triangle: Ni).

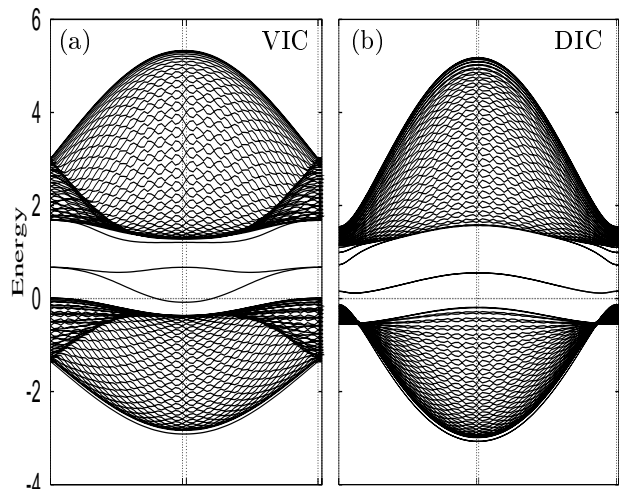


FIG. 3. Dispersion relations for VIC(a) and DIC(b) along the perimeter of the reduced Brillouin zone for $n_h = 0.02$. The chemical potential is at zero. The midgap band is seen in between the AF gap.

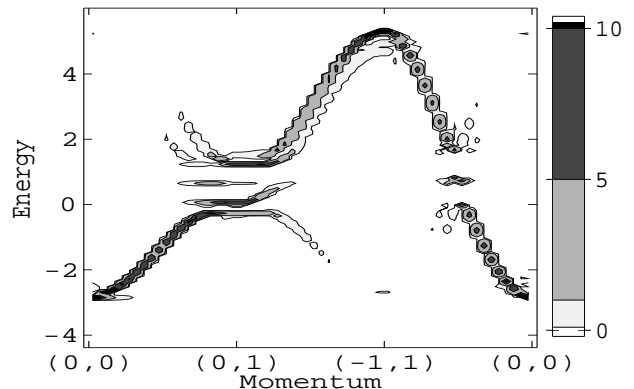


FIG. 4. Contour map of the spectral weight along the symmetry lines in the original Brillouin zone ($n_h = 0.1$ and VIC). The original cosine-like band is hold-backed and gapped to produce the midgap bands and the "shadow" bands at around $\mu = 0$.

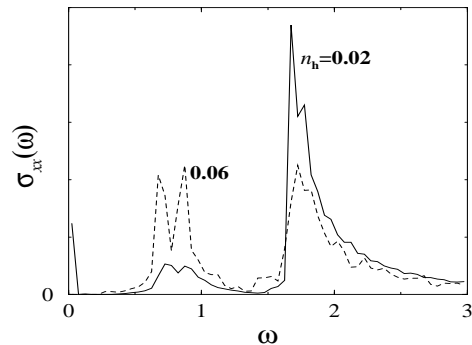


FIG. 5. Optical conductivity (arbitrary units) vs frequency ω in VIC for $n_h = 0.02$ and 0.06 . The midgap absorption at around $\omega \sim 0.8$ grows as doping proceeds.